Double Spin Asymmetries for Large-p_T Hadron Production in Semi-Inclusive DIS

Yuji Koike and J. Nagashima
Department of Physics, Niigata University, Ikarashi, Niigata 950–2181, Japan

Abstract: We study the twist-2 double-spin asymmetries for the 2-jets and large-p_T hadron (π, Λ etc) production in semi-inclusive deep inelastic scattering to $O(\alpha_s)$ in perturbative QCD. After deriving the complete set of the polarized cross section which is differential with respect to the transverse momentum, we discuss characteristic features of the azymuthal spin asymmetries, using existing parton densities and fragmentation functions at COMPASS and EIC energies.

1 Introduction

High energy experiment with polarized beams and targets has opened a new window for revealing QCD dynamics and hadron structures. Ongoing RHIC-SPIN, HERMES and COMPASS experiments are going to provide us with a variety of data disclosing spin distributions inside the nucleon. The planed Electron Ion Collider (EIC) at BNL is expected to be a more powerful and sensitive tool for the QCD spin physics.

In this paper, we study the hadron production in polarized semi-inclusive deep inelastic scattering (SIDIS) off proton. The cross section formula with integrated transverse momentum of the final hadron, p_T, has been derived in the leading order (LO) [1] and in the next-to-leading order (NLO) [2] and has been applied to predict spin asymmetries for polarized Λ production in SIDIS [3]. We extend these studies to derive cross section formula for the complete set of the polarized processes which is differential in p_T and is suited, in particular, for the large-p_T hadron production. This study should be useful to get further insight into the parton densities and fragmentation functions from HERMES, COMPASS and future EIC experiment. It is also complementary to studies on large-p_T hadron production in pp collisions at RHIC and HERA-$\vec{N}$ [4, 5, 6]. As typical SIDIS processes, we study pion (or 2-jets) and Λ hyperon production. In the leading twist-2 level, the complete set of the processes is

$$\begin{aligned}
&\text{(i)} \quad e + p \to e' + \pi(p_T) + X \text{ or } \ e' + 2 \text{ jets} + X, \\
&\text{(ii)} \quad e + \vec{p} \to e' + \vec{\Lambda}(p_T) + X, \\
&\text{(iii)} \quad e + p^\uparrow \to e' + \Lambda^\uparrow(p_T) + X, \\
&\text{(iv)} \quad \vec{e} + \vec{p} \to e' + \pi(p_T) + X \text{ or } \ e' + 2 \text{ jets} + X, \\
&\text{(v)} \quad \vec{e} + p \to e' + \vec{\Lambda}(p_T) + X,
\end{aligned} \tag{1.1}$$

where we have used the notation $\vec{p}$ and $\vec{\Lambda}$ for longitudinally polarized, and $p^\uparrow$ and $\Lambda^\uparrow$ for transversely polarized hadrons, and we restrict ourselves to electron (or muon) scattering off proton. In order that a final hadron carries large transverse momentum, another parton has to be emitted in the opposite direction. This is an $O(\alpha_s)$ effect in perturbative QCD and was investigated in [7, 8] for the unpolarized SIDIS with electron and neutrino beams. Here we extend the analysis to the polarized cases shown above. For small-p_T production in SIDIS, the origin of p_T may be ascribed to the nonperturbative intrinsic transverse momentum of partons confined in or fragementing into a hadron. Derivation of the cross section formula based on this idea was performed in [9], which is complementary to the present study.

As will be shown below, our cross section formula for (i)-(v) applicable in the large-p_T region diverges as $1/p_T^2$ as $p_T \to 0$, which is a manifestation of soft and collinear divergence. For the p_T-integrated cross section, the soft divergence is canceled by the soft divergence in the virtual correction diagrams and the collinear one is factorized into the parton densities.

Accordingly, $O(\alpha_s)$ cross section at $p_T \approx 0$ is to be interpreted as "distribution" with respect to the variable p_T. In order to get a finite p_T-differential cross section, one needs to resum the effect of soft gluon radiation as was studied in [10, 11]. Derivation of the resummed cross section for a low p_T region is beyond the scope of the present study and will be presented elesewhere.

This paper is organized as follows. In section 2 we present the formalism to calculate the cross sections for (1.1) following [8]. Section 3 presents the final analytic formula for the cross section. In Section 4, we present a numerical estimate of the spin asymmetry and discuss its characteristic features, using existing parton distribution and fragmentation functions in the literature. Section 5 is devoted to summary and conclusion.

2 Formalism

In this paper we are interested in the cross section for the process,

$$e(k) + A(p_A, S_A) \to e'(k') + B(p_B, S_B) + X. \tag{2.1}$$

We define 5 Lorentz invariants for specifying the kinematics. The center of mass energy S_{ep} for the initial electron and the proton A is

$$S_{ep} = (p_A + k)^2 \simeq 2p_A \cdot k, \tag{2.2}$$

where we ignored the masses. Conventional DIS variables

$$x_{bj} = \frac{Q^2}{2p_A \cdot q}, \qquad Q^2 = -q^2 = -(k - k')^2, \tag{2.3}$$

are determined by observing the final electron. For the description of kinematics of the final hadron B, we introduce

$$z_f = \frac{p_A \cdot p_B}{p_A \cdot q}, \tag{2.4}$$

and the "transverse" component of q which is orthogonal to p_A and p_B,

$$q_t^\mu = q^\mu - \frac{p_B \cdot q}{p_A \cdot p_B} p_A^\mu - \frac{p_A \cdot q}{p_A \cdot p_B} p_B^\mu. \tag{2.5}$$

q_t is a space-like vector and we define its magnitude as

$$q_T = \sqrt{-q_t^2}. \tag{2.6}$$

Differential cross section for the semi-inclusive production (2.1) can be written as

$$d\sigma = \frac{1}{2S_{ep}} \frac{d^3 p_B}{(2\pi)^3 2p_B^0} \frac{d^3 k'}{(2\pi)^3 2k'^0} \frac{e^4}{q^4} L_{\mu\nu}(k, k') W^{\mu\nu}(p_A, p_B, q), \tag{2.7}$$

where we use the covariant normalization for each state and $1/2S_{ep}$ is the initial flux. $L_{\mu\nu}$ is the leptonic tensor defined as

$$L_{\mu\nu}(k,k') = \frac{1}{2}\mathrm{Tr}\left[\gamma_\mu(1\pm\gamma_5)\not{k}\gamma_\nu\not{k}'\right]$$
$$= 2(k_\mu k'_\nu + k_\nu k'_\mu) - g_{\mu\nu}Q^2 \pm 2i\epsilon_{\mu\nu\lambda\sigma}k^\lambda k'^\sigma. \quad (2.8)$$

with our convention for the anti-symmetric tensor $\epsilon_{0123} = -\epsilon^{0123} = 1$. The leading twist-2 contribution to the hadronic tensor $W^{\mu\nu}$ can be written as

$$W^{\mu\nu}(p_A,p_B,q) = \int_0^1 \frac{dx}{x}\int_0^1 \frac{dz}{z^2}\mathrm{Tr}\left[M_A(x,p_A,S_A)\widehat{M}_B(z,p_B,S_B)H^{\mu\nu}(xp_A,p_B/z,q)\right]$$
$$\times 2\pi\delta\left((xp_A+q-p_B/z)^2\right), \quad (2.9)$$

where $M_A(x,p_A,S_A)$ and $\widehat{M}_B(z,p_B,S_B)$ are the distribution and fragmentation functions for the hadrons A and B, respectively, and $H^{\mu\nu}(xp_A,p_B/z,q)$ is the corresponding hard part. Tr indicates the trace over relevant spinor or Lorentz indices. Since we are interested in the twist-2 cross sections, p_A and p_B can be regarded as light-like. To define the complete set of distribution and fragmentation functions, we introduce another set of light-like vectors n ($n^2=0$) and w ($w^2=0$) for p_A and p_B, respectively, by the relation $p_A\cdot n = 1$ and $p_B\cdot w = 1$. The complete set of the twist-2 quark distribution for the proton A is defined as [12, 13]

$$M^q_{Aij}(x,p_A,S_A) = \int\frac{d\lambda}{2\pi}e^{i\lambda x}\langle p_AS_A|\bar{\psi}_j(0)\psi_i(\lambda n)|p_AS_A\rangle$$
$$= \frac{1}{2}\not{p}_A q(x) + \frac{1}{2}\gamma_5\not{p}_A(S_A\cdot n)\Delta q(x) + \frac{1}{2}\gamma_5\not{S}^\perp_A\not{p}_A\delta q(x) + \cdots, \quad (2.10)$$

and the gluon distrbition is defined as [12, 14, 15]

$$M^{g\alpha\beta}_A(x,p_A,S_A) = \frac{2}{x^2}\int\frac{d\lambda}{2\pi}e^{i\lambda x}\langle p_AS_A|\mathrm{tr}\left[n_\rho G^{\rho\alpha}(0)n_\sigma G^{\sigma\beta}(\lambda n)\right]|p_AS_A\rangle$$
$$= -\frac{1}{2x}G(x)g^{\alpha\beta}_{A\perp} - \frac{1}{2x}\Delta G(x)i\epsilon^{\alpha\beta\rho\sigma}p_{A\rho}n_\sigma + \cdots, \quad (2.11)$$

where $G^{\rho\alpha}$ is the gluon's field strength, tr[ ] means the trace over the color index for $G^{\rho\alpha}$, $g^{\alpha\beta}_{A\perp} = g^{\alpha\beta} - p^\alpha_A n^\beta - n^\alpha p^\beta_A$ and $+\cdots$ stands for the twist-3 or higher. $q(x)$, $\Delta q(x)$ and $\delta q(x)$, respectively, represents spin-average, longitudinally polarized and transversely polarized (transversity) quark distribution. δq is chiral-odd and hence does not mix with gluon distributions. Likewise $G(x)$ and $\Delta G(x)$ are, respectively, spin-average and longitudinally polarized gluon distributions. Notice there is no transversely polarized gluon distribution. Similarly we define twist-2 quark and gluon fragmenation functions for the spin-1/2 hadron

B [12, 16]:

$$\widehat{M}^q_{Bij}(z,p_B,S_B) = \frac{1}{N_c}\int\frac{d\lambda}{2\pi}\,e^{-i\lambda/z}\langle 0|\psi_i(0)|BX\rangle\langle BX|\bar{\psi}(\lambda w)|0\rangle$$

$$= \frac{1}{z}\not{p}_B\widehat{q}(z) + \frac{1}{z}\gamma_5\not{p}_B(S_B\cdot w)\Delta\widehat{q}(z) + \frac{1}{z}\gamma_5\not{S}^\perp_B\not{p}_B\delta\widehat{q}(z) + \cdots, \quad (2.12)$$

$$\widehat{M}^{g\alpha\beta}_B(z,p_B,S_B) = \frac{1}{N_c^2-1}z^2\int\frac{d\lambda}{2\pi}\,e^{-i\lambda/z}\langle 0|\mathrm{tr}[w_\rho G^{\rho\alpha}(0)|BX\rangle\langle BX|w_\sigma G^{\sigma\beta}(\lambda w)]|0\rangle$$

$$= -\widehat{G}(z)g^{\alpha\beta}_{B\perp} - \Delta\widehat{G}(z)i\epsilon^{\alpha\beta\rho\sigma}p_{B\rho}w_\sigma + \cdots, \quad (2.13)$$

with $g^{\alpha\beta}_{B\perp} = g^{\alpha\beta} - p^\alpha_B w^\beta - w^\alpha p^\beta_B$. Physical meaning of each fragmentation function is in parallel with the distribution functions defined above, and we specify them by putting "$\widehat{\ }$" on the corresponding distributions.

For the actual calculation of the cross section, it is convenient to work in the *hadron frame* [8]. In this frame q^μ and p^μ_A take

$$q^\mu = (0,0,0,-Q), \quad (2.14)$$

$$p^\mu_A = \left(\frac{Q}{2x_{bj}},0,0,\frac{Q}{2x_{bj}}\right). \quad (2.15)$$

Choosing the xz-plane as the hadron plane, p_B can be written as

$$p^\mu_B = \frac{z_f Q}{2}\left(1+\frac{q_T^2}{Q^2},\frac{2q_T}{Q},0,\frac{q_T^2}{Q^2}-1\right). \quad (2.16)$$

In order to write the lepton momentum in the hadron frame, we need to introduce the azymuthal angle ϕ between the hadron plane and the lepton plane in the hadron frame. Then the lepton momentum can be parametrized as

$$k^\mu = \frac{Q}{2}\left(\cosh\psi,\sinh\psi\cos\phi,\sinh\psi\sin\phi,-1\right) \quad (2.17)$$

and $k'^\mu = k^\mu - q^\mu$ with

$$\cosh\psi = \frac{2x_{bj}S_{eA}}{Q^2} - 1. \quad (2.18)$$

With these definitions, the cross section for (2.1) can be expressed in terms of S_{ep}, x_{bj}, Q^2, z_f, q_T^2 and ϕ in the hadron frame. Obviously, ϕ is invariant under boost in the q direction, so that the ϕ in the hadron frame is the same, for example, in the center-of-mass system of the virtual photon and the initial proton A. The expression for these variables in terms of the lab. frame variables is given in the Appendix.

Let us proceed to calculate the cross section. As is shown in (2.16) the transverse momentum of p_B is $p_T = z_f q_T$ in the hadron frame, and we shall derive the cross section formula differential in q_T^2. Lowest order diagram in the QCD coupling relevant for the processes (1.1) is shown in Fig. 1. We follow the method of [8] for the calculation. To isolate the ϕ-dependence in the cross section, we first expand the hadronic tensor $W^{\mu\nu}$ in terms of the complete set of the independent tensors. To this end we introduce the following 4 vectors which are orthogonal to each other [8]:

$$
\begin{aligned}
T^\mu &= \frac{1}{Q}\left(q^\mu + 2x_{bj}p_B^\mu\right), \\
X^\mu &= \frac{1}{q_T}\left\{\frac{p_B^\mu}{z_f} - q^\mu - \left(1 + \frac{q_T^2}{Q^2}\right)x_{bj}p_A^\mu\right\}, \\
Y^\mu &= \epsilon^{\mu\nu\rho\sigma} Z_\nu X_\rho T_\sigma, \\
Z^\mu &= -\frac{q^\mu}{Q}.
\end{aligned}
\tag{2.19}
$$

These vectors take the form of $T^\mu = (1,0,0,0)$, $X^\mu = (0,1,0,0)$, $Y^\mu = (0,0,1,0)$, $Z^\mu = (0,0,0,1)$ in the hadron frame, which greatly facilitates the actual calculation presented below. Note that T, X and Z are vectors, while Y is an axial vector. Since $W^{\mu\nu}$ satisfies the current conservation, $q_\mu W^{\mu\nu} = q_\nu W^{\mu\nu} = 0$, it is easy to see that $W^{\mu\nu}$ can be expanded in terms of 9 independent tensors, for which we employ the following:

$$
\begin{aligned}
&\mathcal{V}_1^{\mu\nu} = X^\mu X^\nu + Y^\mu Y^\nu, \quad \mathcal{V}_2^{\mu\nu} = g^{\mu\nu} + Z^\mu Z^\nu, \quad \mathcal{V}_3^{\mu\nu} = T^\mu X^\nu + X^\mu T^\nu, \\
&\mathcal{V}_4^{\mu\nu} = X^\mu X^\nu - Y^\mu Y^\nu, \quad \mathcal{V}_5^{\mu\nu} = i(T^\mu X^\nu - X^\mu T^\nu), \quad \mathcal{V}_6^{\mu\nu} = i(X^\mu Y^\nu - Y^\mu X^\nu), \\
&\mathcal{V}_7^{\mu\nu} = i(T^\mu Y^\nu - Y^\mu T^\nu), \quad \mathcal{V}_8^{\mu\nu} = T^\mu Y^\nu + Y^\mu T^\nu, \quad \mathcal{V}_9^{\mu\nu} = X^\mu Y^\nu + Y^\mu X^\nu.
\end{aligned}
\tag{2.20}
$$

The expansion coefficients of $W^{\mu\nu}$ in terms of these tensors is easily obtained by the inverse tensors $\widetilde{\mathcal{V}}_k$ for $\mathcal{V}_k$ $(k = 1, \cdots 9)$ as

$$
W^{\mu\nu} = \sum_{k=1}^{9} \mathcal{V}_k^{\mu\nu}\left[W_{\rho\sigma}\widetilde{\mathcal{V}}_k^{\rho\sigma}\right], \tag{2.21}
$$

where

$$
\begin{aligned}
&\widetilde{\mathcal{V}}_1^{\mu\nu} = \frac{1}{2}(2T^\mu T^\nu + X^\mu X^\nu + Y^\mu Y^\nu), \quad \widetilde{\mathcal{V}}_2^{\mu\nu} = T^\mu T^\nu, \quad \widetilde{\mathcal{V}}_3^{\mu\nu} = -\frac{1}{2}(T^\mu X^\nu + X^\mu T^\nu), \\
&\widetilde{\mathcal{V}}_4^{\mu\nu} = \frac{1}{2}(X^\mu X^\nu - Y^\mu Y^\nu), \quad \widetilde{\mathcal{V}}_5^{\mu\nu} = \frac{i}{2}(T^\mu X^\nu - X^\mu T^\nu), \quad \widetilde{\mathcal{V}}_6^{\mu\nu} = \frac{-i}{2}(X^\mu Y^\nu - Y^\mu X^\nu),
\end{aligned}
$$

$$\widetilde{\mathcal{V}}_7^{\mu\nu} = \frac{i}{2}(T^\mu Y^\nu - Y^\mu T^\nu), \quad \widetilde{\mathcal{V}}_8^{\mu\nu} = -\frac{1}{2}(T^\mu Y^\nu + Y^\mu T^\nu), \quad \widetilde{\mathcal{V}}_9^{\mu\nu} = \frac{1}{2}(X^\mu Y^\nu + Y^\mu X^\nu). \tag{2.22}$$

Note that $\mathcal{V}_k^{\mu\nu}$ $(k = 1, \cdots, 4, 8, 9)$ are symmetric between μ and ν, and the rest are anti-symmetric. $\mathcal{V}_k^{\mu\nu}$ $(k = 1, \cdots, 5)$ are even under parity, while the rest are odd under parity. For the processes with unpolarized electrons, i.e., (i)-(iii) in (1.1), both $L^{\mu\nu}$ and $W^{\mu\nu}$ are symmetric tensors, accordingly $\mathcal{V}_k^{\mu\nu}$ $(k = 1, \cdots, 4)$ contributes to $W^{\mu\nu}$. For (iv) and (v) both $L^{\mu\nu}$ and $W^{\mu\nu}$ are anti-symmetric pseudo-tensors due to a γ_5 in the trace, accordingly only $\mathcal{V}_k^{\mu\nu}$ $(k = 6, 7)$ contribute to $W^{\mu\nu}$. Actual calculation of $\left[W_{\rho\sigma}\widetilde{\mathcal{V}}_k^{\rho\sigma}\right]$ in (2.21) involves trace over many γ-matrices, which can be carried out conveniently in the hadron frame by using the Tracer program.

With these $\mathcal{V}_k^{\mu\nu}$, we can decompose the ϕ-dependence of the cross sections by the contraction with $L^{\mu\nu}$ in (2.8). Define $\mathcal{A}_k$ $(k = 1, \cdots, 9)$ as

$$\mathcal{A}_k = \frac{1}{Q^2} L_{\mu\nu} \mathcal{V}_k^{\mu\nu} \tag{2.23}$$

then one obtains

$$\begin{aligned}
\mathcal{A}_1 &= 1 + \cosh^2\psi, \\
\mathcal{A}_2 &= -2, \\
\mathcal{A}_3 &= -\cos\phi \sinh 2\psi, \\
\mathcal{A}_4 &= \cos 2\phi \sinh^2\psi, \\
\mathcal{A}_6 &= -2\cosh\psi, \\
\mathcal{A}_7 &= 2\cos\phi \sinh\psi.
\end{aligned} \tag{2.24}$$

From (2.24), the cross section for (i),(ii) and (iii) have ϕ-dependence of 1, $\cos\phi$ and $\cos 2\phi$, while (iv) and (v) have only 1 and $\cos\phi$ dependence.

For the case of (iii) $e + p^\uparrow \to e' + \Lambda^\uparrow + X$, we need to parametrize the spin vector $S_{A\perp}$ and $S_{B\perp}$ which lie in the plane orthogonal to $\vec{p}_A$ and $\vec{p}_B$, respectively. We write

$$S_{A\perp}^\mu = \cos\Phi_A X^\mu + \sin\Phi_A Y^\mu = (0, \cos\Phi_A, \sin\Phi_A, 0), \tag{2.25}$$

$$\begin{aligned}
S_{B\perp}^\mu &= \cos\Theta_B \cos\Phi_B X^\mu + \sin\Phi_B Y^\mu - \sin\Theta_B \cos\Phi_B Z^\mu \\
&= (0, \cos\Theta_B \cos\Phi_B, \sin\Phi_B, -\sin\Theta_B \cos\Phi_B)
\end{aligned} \tag{2.26}$$

where the second equality in each equation follows only in the hadron frame. In the hadron frame, $\Phi_{A,B}$ are the azymuthal angles of $S_{A,B\perp}$ measured from the hadron plane, and Θ_B is

the polar angle of $\vec{p}_B$ measured from the Z-axis which has the Lorentz invariant expression

$$\cos\Theta_B = \frac{q_T^2 - Q^2}{q_T^2 + Q^2}, \qquad \sin\Theta_B = \frac{2q_T Q}{q_T^2 + Q^2}. \tag{2.27}$$

In the Appendix, we present the expression for Φ_A and Φ_B in terms of lab. frame variables.

3 Analytic formula for cross section

By applying the method described in the previous section, we finally obtain the cross section for the large p_T hadron production in DIS in the following form:

$$\frac{d^5\sigma}{dx_{bj}dQ^2dz_f dq_T^2 d\phi} = \frac{\alpha_e^2\alpha_s}{8\pi x_{bj}^2 S_{ep}^2 Q^2}\sum_k \mathcal{A}_k \int_{x_{min}}^1 \frac{dx}{x}\int_{z_f}^1 \frac{dz}{z}\,[f\otimes D\otimes \widehat{\sigma}_k]$$
$$\times\delta\left(\frac{q_T^2}{Q^2} - \left(\frac{1}{\widehat{x}}-1\right)\left(\frac{1}{\widehat{z}}-1\right)\right), \tag{3.1}$$

where $\mathcal{A}_k$ is defined in (2.24), $\alpha_e = e^2/4\pi$ is the QED coupling constant, and we introduced the variables

$$\widehat{x} = \frac{x_{bj}}{x}, \qquad \widehat{z} = \frac{z_f}{z}, \tag{3.2}$$

and

$$x_{min} = x_{bj}\left(1 + \frac{z_f}{1-z_f}\frac{q_T^2}{Q^2}\right). \tag{3.3}$$

For a given S_{ep}, Q^2 and q_T, the kinematic constraint for x_{bj} and z_f is

$$\frac{Q^2}{S_{ep}} < x_{bj} < 1, \tag{3.4}$$

$$0 < z_f < \frac{1-x_{bj}}{1-x_{bj}+x_{bj}q_T^2/Q^2}. \tag{3.5}$$

For a given Q^2, x_{bj} and z_f, q_T can take

$$0 < q_T < Q\sqrt{\left(\frac{1}{x_{bj}}-1\right)\left(\frac{1}{z_f}-1\right)}. \tag{3.6}$$

Roughly speaking, $0 < q_T < Q$ corresponds to the current fragmentation region and $q_T > Q$ corresponds to the target fragmentation region. As is shown in (2.16), the transverse momentum of p_B^μ in the hadron frame is

$$p_T = z_f q_T < z_f Q\sqrt{\left(\frac{1}{x_{bj}}-1\right)\left(\frac{1}{z_f}-1\right)}. \tag{3.7}$$

In (3.1), $[f \otimes D \otimes \widehat{\sigma}_k]$ should read the following form for each process in (1.1) ($C_F = 4/3$):

(i) $e + p \to e' + \{\pi, \Lambda\} + X$ [7]:

$$[f \otimes D \otimes \widehat{\sigma}_k] = \sum_q e_q^2 q(x)\widehat{q}(z)\widehat{\sigma}_k^{qq} + \sum_q e_q^2 G(x)\widehat{q}(z)\widehat{\sigma}_k^{gq} + \sum_q e_q^2 q(x)\widehat{G}(z)\widehat{\sigma}_k^{qg}, \tag{3.8}$$

where

$$\begin{aligned}
\widehat{\sigma}_1^{qq} &= 2C_F\widehat{x}\widehat{z}\left\{\frac{1}{Q^2q_T^2}\left(\frac{Q^4}{\widehat{x}^2\widehat{z}^2} + \left(Q^2 - q_T^2\right)^2\right) + 6\right\}, \\
\widehat{\sigma}_2^{qq} &= 2\widehat{\sigma}_4^{qq} = 8C_F\widehat{x}\widehat{z}, \\
\widehat{\sigma}_3^{qq} &= 4C_F\widehat{x}\widehat{z}\frac{1}{Qq_T}(Q^2 + q_T^2),
\end{aligned} \tag{3.9}$$

$$\begin{aligned}
\widehat{\sigma}_1^{gq} &= \widehat{x}(1-\widehat{x})\left\{\frac{Q^2}{q_T^2}\left(\frac{1}{\widehat{x}^2\widehat{z}^2} - \frac{2}{\widehat{x}\widehat{z}} + 2\right) + 10 - \frac{2}{\widehat{x}} - \frac{2}{\widehat{z}}\right\}, \\
\widehat{\sigma}_2^{gq} &= 2\widehat{\sigma}_4^{gq} = 8\widehat{x}(1-\widehat{x}), \\
\widehat{\sigma}_3^{gq} &= \widehat{x}(1-\widehat{x})\frac{2}{Qq_T}\left\{2(Q^2 + q_T^2) - \frac{Q^2}{\widehat{x}\widehat{z}}\right\},
\end{aligned} \tag{3.10}$$

$$\begin{aligned}
\widehat{\sigma}_1^{qg} &= 2C_F\widehat{x}(1-\widehat{z})\left\{\frac{1}{Q^2q_T^2}\left(\frac{Q^4}{\widehat{x}^2\widehat{z}^2} + \frac{(1-\widehat{z})^2}{\widehat{z}^2}\left(Q^2 - \frac{\widehat{z}^2q_T^2}{(1-\widehat{z})^2}\right)^2\right) + 6\right\}, \\
\widehat{\sigma}_2^{qg} &= 2\widehat{\sigma}_4^{qg} = 8C_F\widehat{x}(1-\widehat{z}), \\
\widehat{\sigma}_3^{qg} &= 4C_F\widehat{x}(1-\widehat{z})^2\frac{1}{\widehat{z}Qq_T}\left\{Q^2 + \frac{\widehat{z}^2q_T^2}{(1-\widehat{z})^2}\right\}.
\end{aligned} \tag{3.11}$$

(ii) $e + \vec{p} \to e' + \vec{\Lambda} + X$:

$$[f \otimes D \otimes \widehat{\sigma}_k] = \sum_q e_q^2 \Delta q(x)\Delta\widehat{q}(z)\Delta_L\widehat{\sigma}_k^{qq} + \sum_q e_q^2 \Delta G(x)\Delta\widehat{q}(z)\Delta_L\widehat{\sigma}_k^{gq} + \sum_q e_q^2 \Delta q(x)\Delta\widehat{G}(z)\Delta_L\widehat{\sigma}_k^{qg}, \tag{3.12}$$

where

$$\Delta_L\widehat{\sigma}_k^{qq} = \widehat{\sigma}_k^{qq} \qquad (k=1,2,3,4), \tag{3.13}$$

$$\begin{aligned}
\Delta_L\widehat{\sigma}_1^{gq} &= \frac{(2\widehat{x}-1)\left\{Q^4(\widehat{x}-1)^2 - q_T^4\widehat{x}^2\right\}}{Q^2q_T^2\widehat{x}(\widehat{x}-1)}, \\
\Delta_L\widehat{\sigma}_2^{gq} &= \Delta_L\widehat{\sigma}_4^{gq} = 0, \\
\Delta_L\widehat{\sigma}_3^{gq} &= \frac{2\left\{Q^2(\widehat{x}-1) - q_T^2\widehat{x}\right\}}{Qq_T},
\end{aligned} \tag{3.14}$$

$$\begin{aligned}
\Delta_L\widehat{\sigma}_1^{qg} &= 2C_F\widehat{x}\widehat{z}\left\{\frac{\widehat{x}-2}{\widehat{x}-1} + \frac{\widehat{x}(\widehat{x}+1)}{(\widehat{x}-1)^2}\frac{q_T^4}{Q^4} + \frac{2(2\widehat{x}^2-2\widehat{x}+1)}{(\widehat{x}-1)^2}\frac{q_T^2}{Q^2}\right\}, \\
\Delta_L\widehat{\sigma}_2^{qg} &= 2\Delta_L\widehat{\sigma}_4^{qg} = 8C_F\frac{\widehat{x}^2\widehat{z}}{\widehat{x}-1}\frac{q_T^2}{Q^2}, \\
\Delta_L\widehat{\sigma}_3^{qg} &= \frac{4C_F\widehat{x}\widehat{z}}{(\widehat{x}-1)^2}\left\{(\widehat{x}-1)^2 + \frac{\widehat{x}^2q_T^2}{Q^2}\right\}\frac{q_T}{Q}.
\end{aligned} \tag{3.15}$$

(iii) $e + p^\uparrow \to e' + \Lambda^\uparrow + X$:
Owing to the chiral-odd nature of the transversity, this process receives a quark contribution only.

$$[f\otimes D\otimes\widehat{\sigma}_k] = \sum_q e_q^2\delta q(x)\delta\widehat{q}(z)\Delta_T\widehat{\sigma}_k^{qq}, \tag{3.16}$$

where

$$\begin{aligned}
\Delta_T\widehat{\sigma}_1^{qq} &= 4C_F\cos(\Phi_A-\Phi_B), \qquad \Delta_T\widehat{\sigma}_2^{qq} = 0, \\
\Delta_T\widehat{\sigma}_3^{qq} &= 4C_F\frac{Q}{q_T}\cos(\Phi_A-\Phi_B), \qquad \Delta_T\widehat{\sigma}_4^{qq} = 4C_F\frac{Q^2}{q_T^2}\cos(\Phi_A-\Phi_B).
\end{aligned} \tag{3.17}$$

(iv) $\vec{e}+\vec{p} \to e' + \{\pi,\Lambda\} + X$:

$$\begin{aligned}
[f\otimes D\otimes\widehat{\sigma}_k] = &\sum_q e_q^2\Delta q(x)\widehat{q}(z)\Delta_{LO}\widehat{\sigma}_k^{qq} + \sum_q e_q^2\Delta G(x)\widehat{q}(z)\Delta_{LO}\widehat{\sigma}_k^{gq} \\
&+ \sum_q e_q^2\Delta q(x)\widehat{G}(z)\Delta_{LO}\widehat{\sigma}_k^{qg},
\end{aligned} \tag{3.18}$$

where

$$\Delta_{LO}\widehat{\sigma}_6^{qq} = -2C_F\left\{\left(\frac{1}{\widehat{x}\widehat{z}}+\widehat{x}\widehat{z}\right)\frac{Q^2}{q_T^2}-\frac{\widehat{x}\widehat{z}q_T^2}{Q^2}\right\},$$

$$\Delta_{LO}\widehat{\sigma}_7^{qq} = -4C_F\widehat{x}\widehat{z}\frac{Q^2-q_T^2}{Qq_T}, \tag{3.19}$$

$$\Delta_{LO}\widehat{\sigma}_6^{gq} = -\frac{2\widehat{x}-1}{\widehat{x}}\left(2\widehat{x}+\frac{\widehat{x}-1}{\widehat{z}^2}\frac{Q^2}{q_T^2}\right),$$

$$\Delta_{LO}\widehat{\sigma}_7^{gq} = -\frac{2Q}{q_T}\frac{(\widehat{x}-1)(2\widehat{z}-1)}{\widehat{z}}, \tag{3.20}$$

$$\Delta_{LO}\widehat{\sigma}_6^{qg} = \frac{2C_F\widehat{z}}{\widehat{x}-1}\left\{\frac{1}{\widehat{z}^2}-(\widehat{x}-1)^2+\frac{\widehat{x}^4}{(\widehat{x}-1)^2}\frac{q_T^4}{Q^4}\right\},$$

$$\Delta_{LO}\widehat{\sigma}_7^{qg} = \frac{4C_F\widehat{x}\widehat{z}}{\widehat{x}-1}\left(1-\frac{\widehat{x}}{\widehat{z}}\right)\frac{q_T}{Q}. \tag{3.21}$$

(v) $\vec{e}+p\to e'+\vec{\Lambda}+X$:

$$[f\otimes D\otimes\widehat{\sigma}_k] = \sum_q e_q^2 q(x)\Delta\widehat{q}(z)\Delta_{OL}\widehat{\sigma}_k^{qq}+\sum_q e_q^2 G(x)\Delta\widehat{q}(z)\Delta_{OL}\widehat{\sigma}_k^{gq}$$
$$+\sum_q e_q^2 q(x)\Delta\widehat{G}(z)\Delta_{OL}\widehat{\sigma}_k^{qg}, \tag{3.22}$$

where

$$\Delta_{OL}\widehat{\sigma}_{6,7}^{qq} = \Delta_{LO}\widehat{\sigma}_{6,7}^{qq}, \tag{3.23}$$

$$\Delta_{OL}\widehat{\sigma}_6^{gq} = \frac{2\widehat{x}^2-2\widehat{x}+1}{\widehat{x}\widehat{z}}\left(\widehat{x}+(\widehat{x}-1)\frac{Q^2}{q_T^2}\right),$$

$$\Delta_{OL}\widehat{\sigma}_7^{gq} = \frac{2Q}{q_T}\frac{(\widehat{x}-1)(2\widehat{x}-1)}{\widehat{z}}, \tag{3.24}$$

$$\Delta_{OL}\widehat{\sigma}_6^{qg} = \frac{2C_F\widehat{z}}{\widehat{x}-1}\left\{\frac{1}{\widehat{z}^2}+(\widehat{x}-1)^2-\frac{\widehat{x}^4}{(\widehat{x}-1)^2}\frac{q_T^4}{Q^4}\right\},$$

$$\Delta_{OL}\widehat{\sigma}_7^{qg} = -\frac{4C_F\widehat{x}\widehat{z}}{\widehat{x}-1}\left(1-\frac{\widehat{x}}{\widehat{z}}\right)\frac{q_T}{Q}. \tag{3.25}$$

Several comments are in order here:

(1) From the above formula one can separate the ϕ-dependence of the q_T-differential cross section for (i)-(v) in (1.1) as

$$\frac{d\sigma}{dQ^2 dx_{bj} dz_f dq_T^2 d\phi} = \sigma_0 + \cos(\phi)\sigma_1 + \cos(2\phi)\sigma_2, \tag{3.26}$$

with $\sigma_2 \equiv 0$ for (iv) and (v). Transverse momentum of partons also gives the same ϕ dependence as a purely kinematic effect [17]. It is, however, interesting to test whether the above $0(\alpha_s)$ formula gives quantitatively right magnitude for each component.

(2) The cross section depends on S_{ep} through $\mathcal{A}_k$ in (2.24). For $x_{bj}S_{ep}/Q^2 >> 1$ (see (2.18), we have $\mathcal{A}_{1,3,4} >> \mathcal{A}_{6,7}$ (ϕ-dependence factored out), which results in the strong suppression of the asymmetry for (iv) and (v) compared to (ii) and (iii) in (1.1).

(3) In the large-q_T SIDIS, contribution from the gluon distribution and fragmentation functions is of the same $O(\alpha_s)$ effect as the quark contibution, so that q_T-differential cross section is expected to be a more sentitive tool to determine detailed form of the polarized gluon contibution than the q_T-integrated case [8].

(4) Except for (iii), σ_0 has a nonintegrable $1/q_T^2$-dependence at $q_T \to 0$, while $\sigma_{1,2}$ are integrable. For the case of transverse polarization (iii), σ_2 has the $1/q_T^2$-dependence, while $\sigma_{0,1}$ is integrable at $q_T \to 0$. To get a finite meaningful result for all value of q_T, one needs to include higher order effect based on the resummation technique as in the case of the spin-average case [10, 11].

4 Numerical estimate

4.1 Azymuthal asymmetry

In this section, we present a numerical estimate of the polarized cross sections (ii)-(v) in (1.1) in comparison with the spin averaged one (i), using the exisiting parton distributions for the nucleon and the fragmentation function for pion and Λ. For this purpose we consider the azymuthal asymmetries defined as follows:

$$\langle 1 \rangle_{S_A S_B} \equiv \frac{\int_0^{2\pi} d\phi \frac{d^5\sigma^{pol}}{dQ^2 dx_{bj} dz_f dq_T^2 d\phi}}{\int_0^{2\pi} d\phi \frac{d^5\sigma^{av}}{dQ^2 dx_{bj} dz_f dq_T^2 d\phi}} = \frac{\sigma_0^{pol}}{\sigma_0^{av}},$$

$$\langle \cos(n\phi) \rangle_{S_A S_B} \equiv \frac{\int_0^{2\pi} d\phi \cos(n\phi) \frac{d^5\sigma^{av,pol}}{dQ^2 dx_{bj} dz_f dq_T^2 d\phi}}{\int_0^{2\pi} d\phi \frac{d^5\sigma^{av}}{dQ^2 dx_{bj} dz_f dq_T^2 d\phi}} = \frac{\sigma_n^{av,pol}}{2\sigma_0^{av}}, \qquad (n = 1, 2) \tag{4.1}$$

where σ^{av} and σ^{pol} are the spin-averaged and polarized cross sections and their decomposition $\sigma_{0,1,2}^{av,pol}$ is defined in (3.26). The subscript $S_A S_B$ in the left-hand-side of (4.1) specify

the spin states of the hadrons A and B for each process in (1.1). We use the symbol O for spin-average, L for longitudinal polarization and T for transverse polarization. Accordingly, $S_A S_B$ in (4.1) can be $S_A S_B = LL,\ TT,\ LO,\ OL$ corresponding to (ii), (iii), (iv) and (v), respectively. By definition $\langle 1\rangle_{OO} \equiv 1$. For all cases, $|\langle 1\rangle_{S_A S_B}| < 1$ and $|\langle \cos(n\phi)\rangle_{S_A S_B}| < 1$.

The asymmetries (4.1) are still functions of 5 variables, S_{ep}, Q^2, x_{bj}, z_f and q_T. We estimate them at COMPASS ($S_{ep} = 300$ GeV^2) and EIC ($S_{ep} = 10^4$ GeV^2) energies with typical kinematic variables where our perturbative formula are valid. Comparison of predicted asymmetries with experimental data may be better achieved by integrating over some of the variables to gain statistics. Here we will not try this procedure, but will show the nonintegrated azymuthal asymmetry, intending to show a typical dependence of the asymmetry on each variable. To determine the kinematic variables, we first note from (2.18) and (2.24) that at large $\cosh\psi = 2x_{bj}S_{ep}/Q^2 - 1$, the spin asymmetry for (iv) and (v) is strongly suppressed compared with (ii) and (iii), so that a smaller value of x_{bj} is prefered. In addition, if one chooses the same values of Q^2 and $\cosh\psi$ at COMPASS and EIC energies, variation of the asymmetry at different x_{bj} is wholly ascribed to the variation of distribution and/or fragmentation functions and the partonic hard cross sections. Keeping this in mind we have chosen $(Q^2, x_{bj}) = (100\text{GeV}^2, 0.4)$ for the COMPASS energy and $(Q^2, x_{bj}) = (100\text{GeV}^2, 0.012)$ for the EIC energy, by which "valence" and "sea" region of the parton densities are mainly probed.

As a reference distribution and fragmentation functions, we use GRV parton density for the unpolarized nucleon [18], GRSV polarized parton density [19], KKP fragmentation function for $\pi^+ + \pi^-$ [20] and FSV Λ-fragmentation function [3] for polarized and unpolarized $\Lambda + \bar{\Lambda}$. In all cases we use NLO versions, putting the factorization scale $\mu_F^2 = Q^2$.

4.2 Pion or 2-jets production

The process (iv) $\vec{e} + \vec{p} \to e' + 2$ jets $+ X$ or $e' + \pi + X$ may be useful to get further insight into the polarized parton distribution in the nucleon. Here we present an estimate of $\langle 1\rangle_{LO}$ and $\langle \cos\phi\rangle_{LO}$ for the charged pion production. Figure 2 shows the q_T-dependence ((a) and (b)) and z_f-dependence ((c) and (d)) of these asymmetries at COMPASS ((a) and (c)) and EIC ((b) and (d)) kinematics. $\langle \cos\phi\rangle_{OO}$ is also shown for comparison. For the spin asymmetry, we showed the results with standard (solid line) and valence (dashed line) scenarios in the GRSV distribution. At $x_{bj} = 0.4$, the spin asymmetry $\langle 1\rangle_{LO}$ can be as large as 50 %, while $\langle \cos\phi\rangle_{LO}$ is within a few % level. At $x_{bj} = 0.012$, these magnitudes are somewhat reduced, since the polarized parton density is more suppressed in the small x-region compared to the unpolarized parton density. At $x_{bj} = 0.4$, the two scenarios give totally different behavior for $\langle 1\rangle_{LO}$, which can be, in principle, a sensitive test for the polarized parton density. Typical magnitude of $\langle \cos\phi\rangle_{OO}$ is larger than $\langle \cos\phi\rangle_{LO}$ as expected, since the unpolarized parton density is larger than the polarized one.

4.3 Λ production

Figure 3 shows the q_T-dependence ((a) and (b)) and the z_f-dependence ((c) and (d)) of the azymuthal spin asymmetry for (v) $\vec{e}+p \to e'+\vec{\Lambda}+X$ ((a) and (c) for $\langle 1\rangle_{OL}$, and (b) and (d) for $\langle \cos\phi\rangle_{OL}$) at the COMPASS kinematics. Figure 4 shows the same asymmetries as Fig. 3 but for the EIC kinematics. In [3], three sets of polarized fragmentation function for $\Lambda+\bar{\Lambda}$ have been constructed based on three different assumptions at a low energy input scale: Scenario 1 corresponds to the nonrelativstic quark model picture, where only polarized s-quark is assumed to fragment into the polarized Λ, i.e., $\Delta\widehat{u} = \Delta\widehat{d} = 0$. Scenario 2 is based on the assumption that the Λ fragmentation function has the same flavor decomposition as the Λ distribution function constructed from proton's structure function g_1^p by the $SU(3)$ flavor symmetry, i.e., $-\Delta\widehat{u} = -\Delta\widehat{d} = 0.2\Delta\widehat{s}$. Scenario 3 assumes three flavors contribute equally to the fragmentation process, i.e., $\Delta\widehat{u} = \Delta\widehat{d} = \Delta\widehat{s}$. In all three cases, $\Delta\widehat{s}$ has positive sign. We calculated the asymmetries with these three sets. In both kinematics, $\langle 1\rangle_{OL}$ can be as large as 50 %, while $\langle \cos\phi\rangle_{OL}$ is within a few % level, varying with different scenarios for the Λ fragmentation functions.

The pattern of the calculated asymmetry $\langle 1\rangle_{OL}$ can be easily understood [3]. At the COMPASS kinematics with $x_{bj} = 0.4$, contribution to the asymmetry is basically from the valence u-quark distribution (see (3.1) and (3.3)). Thus scenario 1 in which only s-quark fragments into $\vec{\Lambda}$ gives negligible asymmetry, while scenarios 2 and 3 gives, respectively, negative and positive asymmetries, the former being smaller in magnitude. At the EIC kinematics with smaller x_{bj} ($x_{bj} = 0.012$), a large contribution comes from the sea-quark distribution, which is nearly flavor symmetric. Accordingly scenario 1 also gives a positive asymmetry with its magnitude smaller than the scenario 3, since only s-quark fragments into $\vec{\Lambda}$. In scenario 2, u and d quark contribution is partially canceled by s-quark contribution, resulting in the small negative asymmetry.

Figures 5 and 6 show the asymmetry for (ii) $e + \vec{p} \to e' + \vec{\Lambda} + X$ at the COMPASS and EIC kinematics, respectively. We show the results with the standard scenario for the GRSV polarized parton density. For comparison unpolarized azymuthal asymmetry $\langle \cos\phi\rangle_{OO}$ and $\langle \cos 2\phi\rangle_{OO}$ are also shown in Fig. 5, the former being essentially the same as the one for the pion production shown in Fig. 2 as expected. Typical magnitude of $\langle 1\rangle_{LL}$, $\langle \cos\phi\rangle_{LL}$ and $\langle \cos 2\phi\rangle_{LL}$ at $x_{bj} = 0.4$ is a few 10 %, a few %, and $O(10^{-3})$. At $x_{bj} = 0.4$, $\langle 1\rangle_{LL}$ and $\langle \cos\phi\rangle_{LL}$ have approximately the same magnitude as $\langle 1\rangle_{OL}$ and $\langle \cos(\phi)\rangle_{OL}$. At $x_{bj} = 0.012$, $\langle 1\rangle_{LL}$ and $\langle \cos\phi\rangle_{LL}$ are, respectively, smaller than $\langle 1\rangle_{OL}$ and $\langle \cos\phi\rangle_{OL}$, since polarized parton density is more suppressed at smaller x region compared with unpolarized parton density. The distinction among three scenarios for the polarized Λ fragmentation function can be understood in the same way as the asymmetry for (v) $\vec{e}+p \to e' + \vec{\Lambda} + X$ shown in Figs. 3 and 4.

Figures 7 and 8 show the spin asymmetry for (iii) $e+p^\uparrow \to e'+\Lambda^\uparrow+X$ at the COMPASS and EIC kinematics. The calculation is done at $\cos(\Phi_A - \Phi_B) = 1$. In the present estimate, we assume the transversity distribution and the trasversity fragmentation function are equal to the longitudinally polarized distribution and fragmentation function, respectively: We put $\delta q \equiv \Delta q$ and $\delta\widehat{q} \equiv \Delta\widehat{q}$. This assumption may be justified at a low energy scale.

But even in that case, they should be different at high energy, since their Q^2-evolution is different, in particular, at small x [21]. One can alternatively estimate the upper bound based on the Soffer's equality as was done for $p^\uparrow + p \to \Lambda^\uparrow + X$ [5]. Here we intend to present a simplest estimate to study characteristic features of the asymmetry by the above ansatz. One sees from the figures that $\langle 1\rangle_{TT}$ is of a few % $\sim$ 20 % at $x_{bj} = 0.4$ depending on the scenarios for the Λ fragmentation function. This value is smaller than $\langle 1\rangle_{LL}$, which is expected since there is no gluon contribution to the transverse spin asymmetry. On the other hand, $\langle \cos\phi\rangle_{TT}$ is from a few to 10 %, and even $\langle \cos 2\phi\rangle_{TT}$ is of a few % level, which are much larger than $\langle \cos n\phi\rangle_{LL}$ $(n = 1, 2)$. The same feature persists also at $x_{bj} = 0.012$, although absolute magnitude of the asymmetry becomes smaller by the same reason for $\langle \cos n\phi\rangle_{LL}$ $(n = 0, 1, 2)$. It is interesting to check these peculiar features of the hard cross section in future experiments and to get information about transversity.

5 Summary and conclusion

In this paper, we have studied the double spin asymmeties for 2-jets and large-p_T hadron production in semi-inclusive DIS with one-photon exchange. The cross section formula for the complete set of the spin dependent processes (1.1) has been derived to $O(\alpha_s)$. Separating the dependence on the azymuthal angle ϕ between the hadron and lepton planes, the formula can be written as

$$\frac{d^5\sigma}{dx_{bj}dQ^2dz_f dq_T^2 d\phi} = \sigma_0 + \cos\phi\,\sigma_1 + \cos 2\phi\,\sigma_2, \tag{5.1}$$

where the last term is absent for the process with polarized lepton beams. This decomposition is purely kinematic, while the magnitude of each component depends on the origin of the transverse momentum of the final hadron. At low p_T, nonperturbative component such as intrinsic-k_T of partons is expected to contribute as studied in [9]. At moderate p_T, higher order effect represented by the resummed cross section is presumably important. Our $O(\alpha_s)$ formula should be useful to clarify the importance of these effects and to see at which p_T the experimentally observed spin asymmetry follows the perturbative QCD prediction.

In order to see the qualitative behavior of each component in (5.1), we calculated the azymuthal asymmetries using the parton distribution for the nucleon and the fragmentation functions for π and Λ at $x_{bj} = 0.4$ and $x_{bj} = 0.012$. We found that the asymmetry is very sensitive to different scenarios of parton distribution and fragmentation functions as was expected from the previous studies on SIDIS and pp collisions [3, 4, 5]. Typical magnitude of asymmetry from each component in (5.1) turns out to be $O(0.1 \sim 0.6)$, $O(10^{-2})$ and $O(10^{-3})$ from the first to third term in (5.1). For the process (iii) $e + p^\uparrow \to e' + \Lambda^\uparrow + X$ in (1.1), however, the second and third contribution in (5.1) is significantly larger, while the first term is smaller, compared with other spin asymmetries.

As in the case of unpolarized cross sections, σ_0 component of the polarized cross sections have $1/q_T^2$-singularity at low q_T, except for the above process (iii) where σ_2 has the same

singularity. To get a meaningful formula at low q_T, we need resummation technique [10, 11], which will be reported in a future publication.

Acknowledgement:

This work is supported in part by the Grant-in-Aid for Scientific Research of Monbu-Kagaku-sho.

Appendix

In this appendix, we give the expression for the Lorentz invariants and hadron frame variables in terms of the variables in the Lab. frame. (See [8] for the detail.) In the Lab. frame, 4-vectors which appeared in the text can be parametrized as

$$\begin{aligned}
p_A^\mu &= E_A(1,0,0,1),\\
p_B^\mu &= E_B(1,\sin\theta_B\cos\phi_B,\sin\theta_B\sin\phi_B,\cos\theta_B),\\
k^\mu &= E(1,0,0,-1),\\
k'^\mu &= E'(1,-\sin\theta,0,-\cos\theta),\\
q^\mu &= (E-E',E'\sin\theta,0,E'\cos\theta-E),\\
S_{A\perp}^\mu &= (0,\cos\Phi_A^L,\sin\Phi_A^L,0),\\
S_{B\perp}^\mu &= (0,\cos\theta_B\cos\phi_B\cos\Phi_B^L-\sin\phi_B\sin\Phi_B^L,\\
&\qquad \cos\theta_B\sin\phi_B\cos\Phi_B^L+\cos\phi_B\sin\Phi_B^L,-\sin\theta_B\cos\Phi_B^L),
\end{aligned} \tag{A.1}$$

where $\Phi_{A,B}^L$ is the azymuthal angle of the transverse spin vector $S_{A,B\perp}$ which satisfy $\vec{S}_{A\perp}\cdot\vec{p}_A=\vec{S}_{B\perp}\cdot\vec{p}_B=0$. In order to give the expression for q_T^2, we introduce the polar angle θ_* for p_B in the Born amplitude (diagram obtained by removing the gluon line from Fig.1(a)), which allows us to write $p_B\propto(1,\sin\theta_*,0,\cos\theta_*)$. It is easy to show θ_* is given as

$$\cot\frac{\theta_*}{2}=\frac{2x_{bj}E_A}{Q}\sqrt{1-\frac{Q^2}{x_{bj}S_{ep}}}. \tag{A.2}$$

With this θ_* we have

$$q_T^2=\frac{8E^2-4E'(2E-E')(1+\cos\theta)}{1-\cos\theta_B}\left\{\sin^2\left((\theta_B-\theta_*)/2\right)+\sin\theta_B\sin\theta_*\sin^2\left(\phi_B/2\right)\right\}, \tag{A.3}$$

and

$$\cos\phi=\frac{Q}{2q_T}\left(1-\frac{Q^2}{x_{bj}S_{ep}}\right)^{-1/2}\left\{1-\frac{Q^2}{x_{bj}S_{ep}}+\frac{q_T^2}{Q^2}-\left(\frac{Q}{2x_{bj}E_A}\right)^2\cot^2(\theta_B/2)\right\}. \tag{A.4}$$

Finally, the azymuthal angles $\cos\Phi_A$ and $\cos\Phi_B$ in the hadron frame can be written as

$$\cos\Phi_A = -S_{A\perp}\cdot X = \frac{1}{q_T}\left(\frac{1}{z_f}E_B\sin\theta_B\cos(\phi_B-\Phi_A^L) - E'\sin\theta\cos\Phi_A^L\right), \qquad (A.5)$$

$$\begin{aligned}\cos\Phi_B &= \frac{1}{\sin\Theta_B}S_{B\perp}\cdot Z \\ &= \frac{Q^2+q_T^2}{2Q^2q_T}\Big\{E'\sin\theta\left(\cos\phi_B\cos\theta_B\cos\Phi_B^L - \sin\phi_B\sin\Phi_B\right) \\ &\qquad -(E'\cos\theta - E)\sin\theta_B\cos\Phi_B^L\Big\}. \end{aligned} \qquad (A.6)$$

References

[1] X. Ji, Phys. Rev. **D49** (1994) 114.

[2] D. de Florian, C.A. Garcia Canal and R. Sassot, Nucl. Phys. **B470** (1996) 195; D. de Florian and R. Sassot, Nucl. Phys. **B488** (1997) 367.

[3] D. De Florian, M. Stratmann and W. Vogelsang, Phys. Rev. **D63** (1998) 5811.

[4] D. De Florian, M. Stratmann and W. Vogelsang, Phys. Rev. Lett. **81** (1998) 530.

[5] D. De Florian, J. Soffer, M. Stratmann and W. Vogelsang, Phys. Lett. **B439** (1998) 176.

[6] C. Boros, J.T. Londergan and A.W. Thomas, Phys. Rev, **D62** (2000) 014021.

[7] A. Méndez, Nucl. Phys. **B145** (1978) 199.

[8] R. Meng, F.I. Olness and D. Soper, Nucl. Phys. **B371** (1992) 79.

[9] P.J. Mulders and R.D. Tangerman, Nucl. Phys. **B461** (1996) 197.

[10] R. Meng, F.I. Olness and D. Soper, Phys. Rev. **D54** (1996) 1919.

[11] P.M. Nadolsky, D.R. Stump and C.P. Yuan, Phys. Rev. **D61** (2000) 014003.

[12] J.C. Collins and D. Soper, Nucl. Phys. **B194** (1982) 445.

[13] R.L. Jaffe and X. Ji, Nucl. Phys. **B375** (1992) 527.

[14] A.V. Manohar, Phys. Rev. Lett. **65** (1990) 2511.

[15] X. Ji, Phys. Lett. **B289** (1992) 137.

[16] R.L. Jaffe and X. Ji, Phys. Rev. Lett. **71** (1993) 2547.

[17] R.N. Cahn, Phys. Lett. **B78** (1978) 269.

[18] M. Glück, E. Reya and A. Vogt, Eur. Phys. J. **C5** (1998) 461.

[19] M. Glück, E.Reya, M. Stratmann and W. Vogelsang, Phys. Rev. **D63** (2001) 094005.

[20] B.A. Kniehl, G. Kramer and B. Pötter, Nucl. Phys. **B582** (2000) 514.

[21] X. Artru and M. Mekhfi, Z. Phys. **C45** (1990) 669;
W. Vogelsang, Phys. Rev. **D57** (1998) 1886;
A. Hayashigaki, Y. Kanazawa and Y. Koike, Phys. Rev. **D56** (1997) 7350.

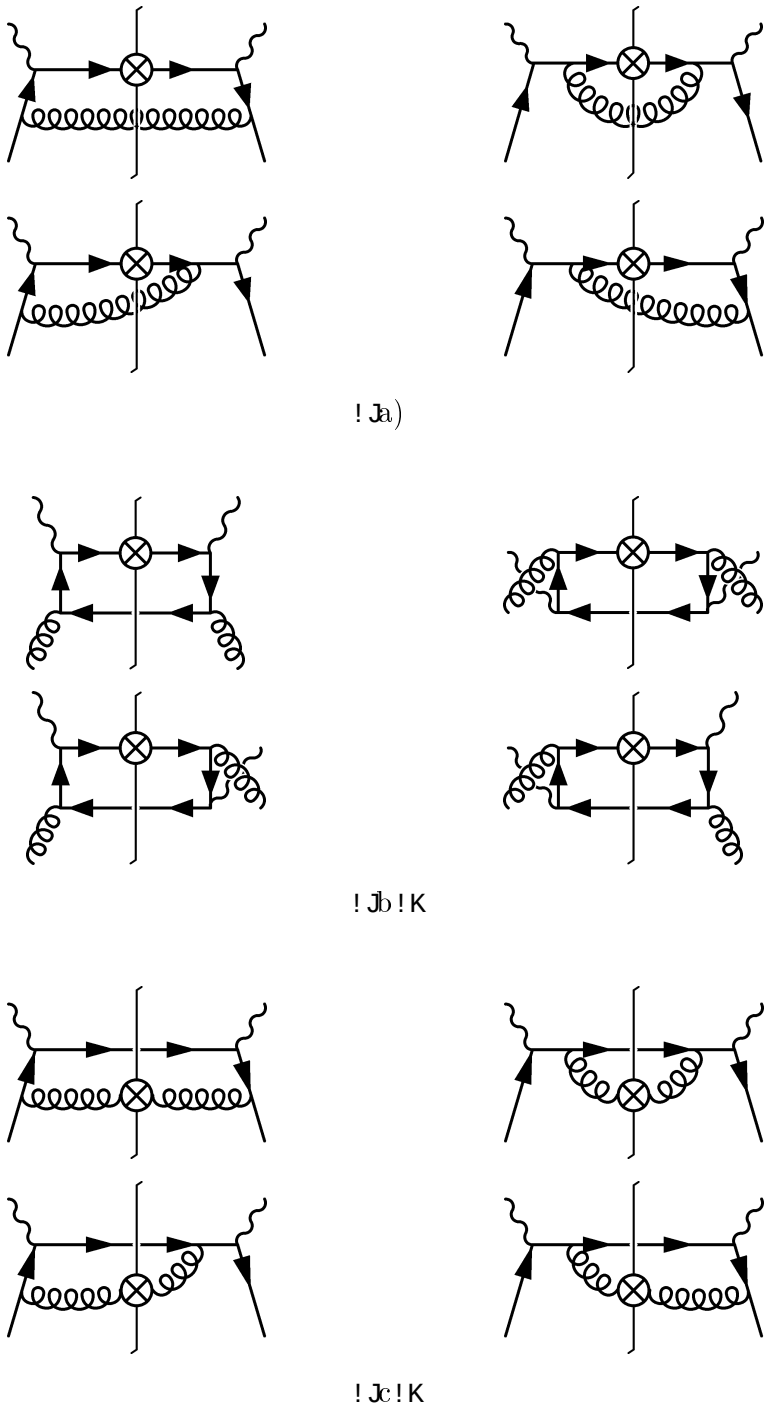

Figure 1: $O(\alpha_s)$ cut diagrams contributing to large p_T hadron production in SIDIS. Distribution function is located in the lower part of each diagram, and $\otimes$ show the fragmentation function insertion.

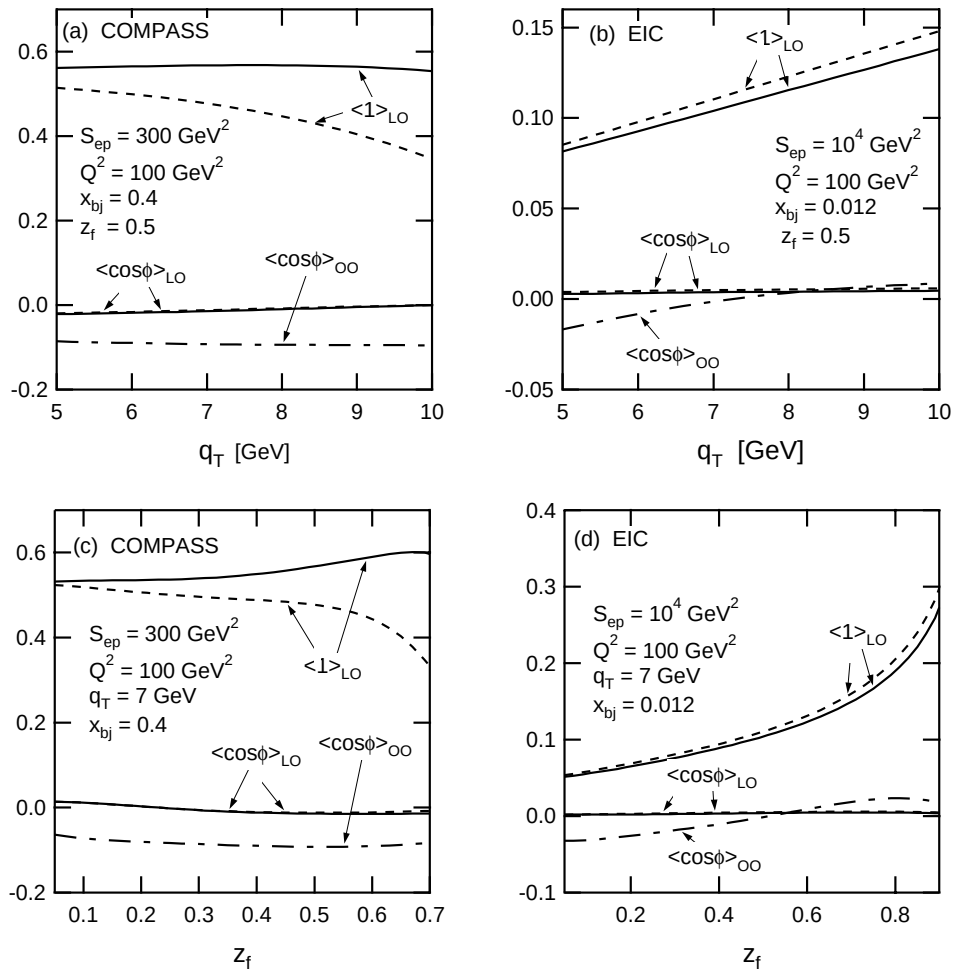

Figure 2: Azymuthal spin asymmetry for the pion production $\vec{e}+\vec{\pi} \to e'+\pi+X$. (a) and (b) show the q_T-dependence of the asymmetry at COMPASS and EIC energies, respectively. (c) and (d) show the z_f-dependence of the asymmetry at COMPASS and EIC energies, respectively. Solid- and dashed- lines, respectively, denote those obtained with standard- and valence- scenarios of GRSV polarized parton density. Dash-dot lines denotes Azymuthal asymmetry $\langle \cos\phi \rangle_{OO}$ for the unpolarized cross section.

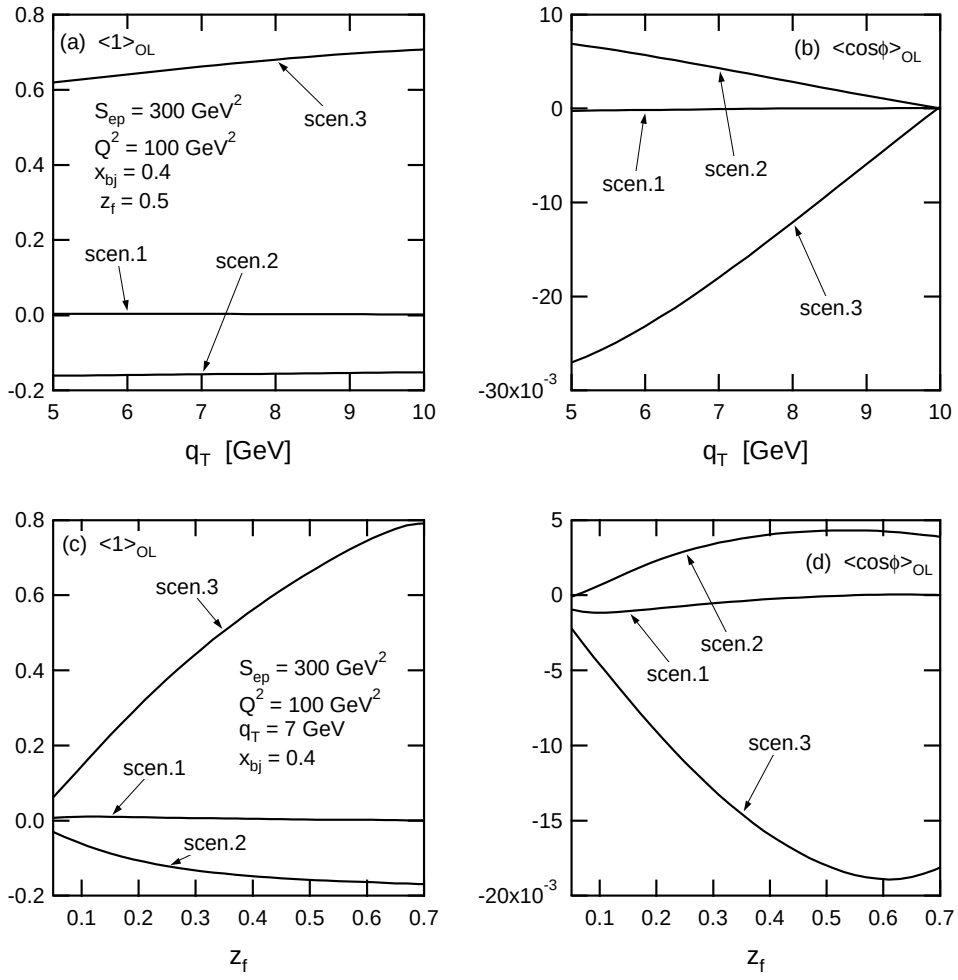

Figure 3: Azymuthal spin asymmetry for $\vec{e}+p \to e' + \vec{\Lambda} + X$ at the COMPASS energy. (a) and (b) show the q_T-dependence of $\langle 1 \rangle_{OL}$ and $\langle \cos\phi \rangle_{OL}$, respectively. (c) and (d) show the z_f-dependence of $\langle 1 \rangle_{OL}$ and $\langle \cos\phi \rangle_{OL}$, respectively.

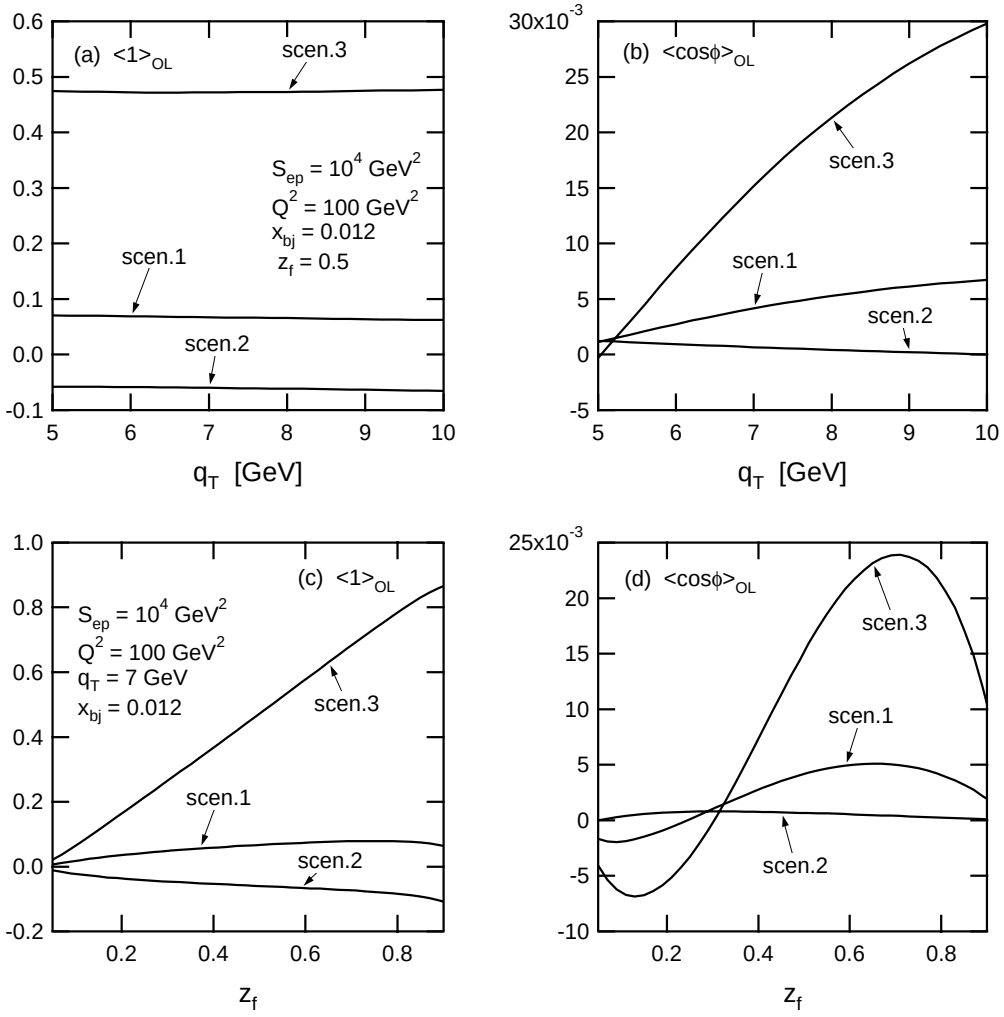

Figure 4: The same as Fig. 3 but for EIC energy.

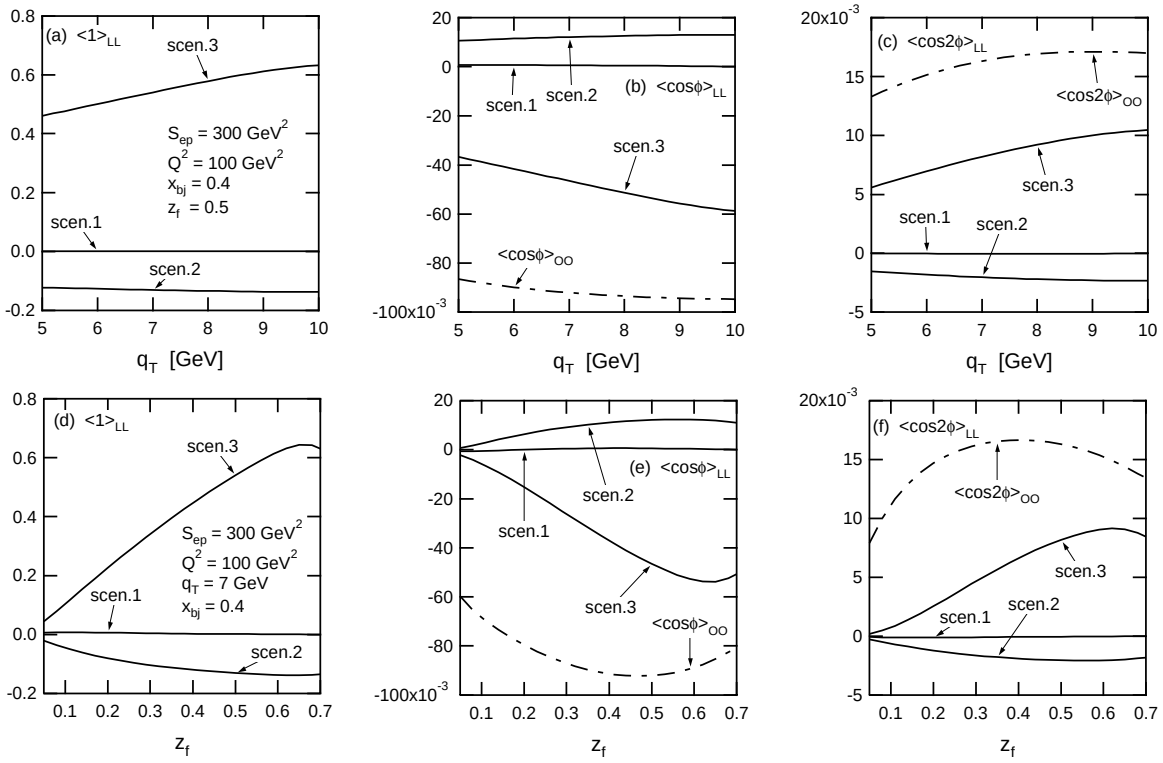

Figure 5: Azymuthal spin asymmetry for $e + \vec{p} \to e' + \vec{\Lambda} + X$ at the COMPASS energy. (a),(b) and (c) show the q_T-dependence of $\langle 1 \rangle_{LL}$, $\langle \cos\phi \rangle_{LL}$ and $\langle \cos 2\phi \rangle_{LL}$, respectively. (d),(e) and (f) show the z_f-dependence of $\langle 1 \rangle_{LL}$, $\langle \cos\phi \rangle_{LL}$ and $\langle \cos 2\phi \rangle_{LL}$, respectively. Unpolarized azymuthal asymmetry $\langle \cos\phi \rangle_{OO}$ is shown in (b) and (e), and $\langle \cos 2\phi \rangle_{OO}$ is shown in (c) and (f) for comparison.

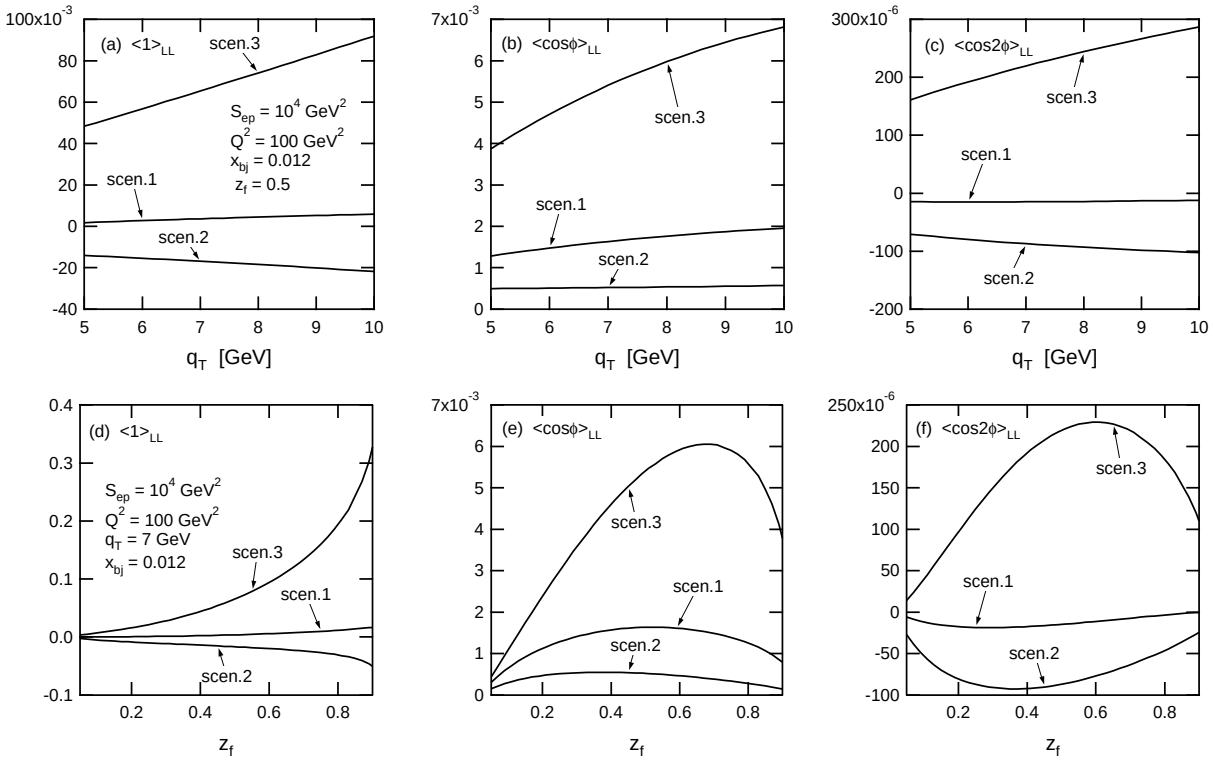

Figure 6: The same as Fig. 5 but for EIC energy.

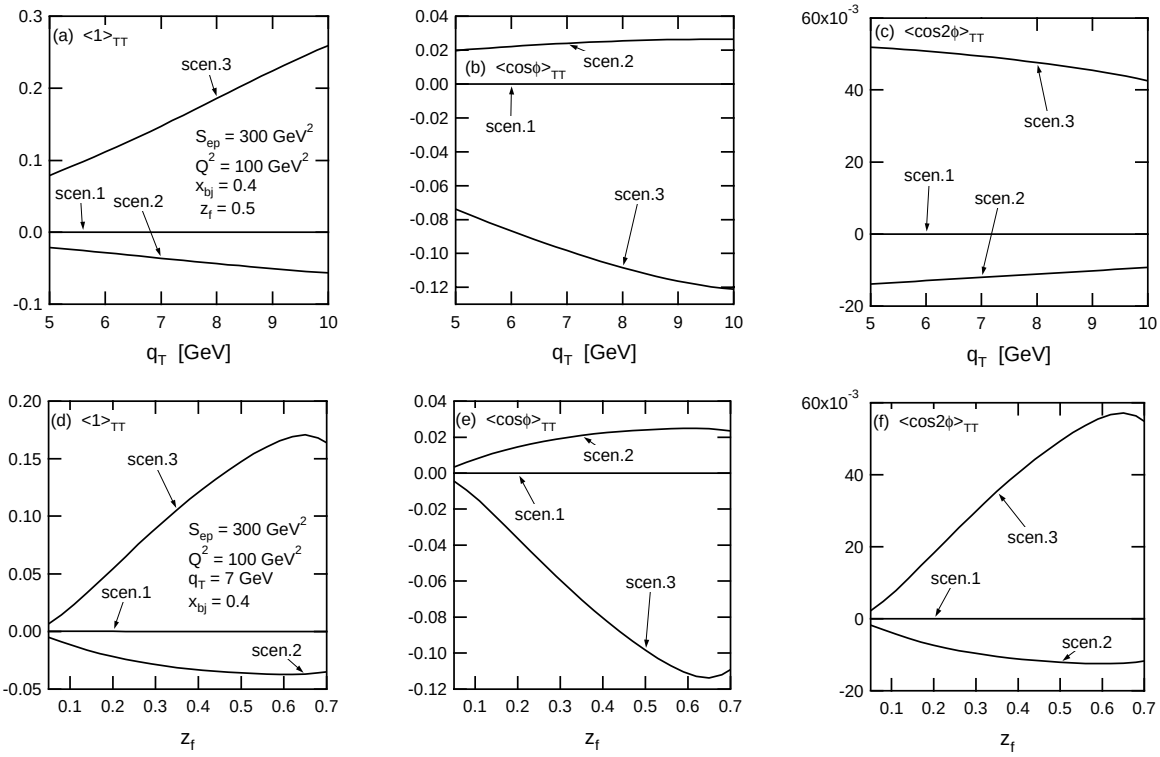

Figure 7: Azymuthal spin asymmetry for $e + p^{\uparrow} \to e' + \Lambda^{\uparrow} + X$ at the COMPASS energy. (a),(b) and (c) show the q_T-dependence of $\langle 1 \rangle_{TT}$, $\langle \cos\phi \rangle_{TT}$ and $\langle \cos 2\phi \rangle_{TT}$, respectively. (d),(e) and (f) show the z_f-dependence of $\langle 1 \rangle_{TT}$, $\langle \cos\phi \rangle_{TT}$ and $\langle \cos 2\phi \rangle_{TT}$, respectively.

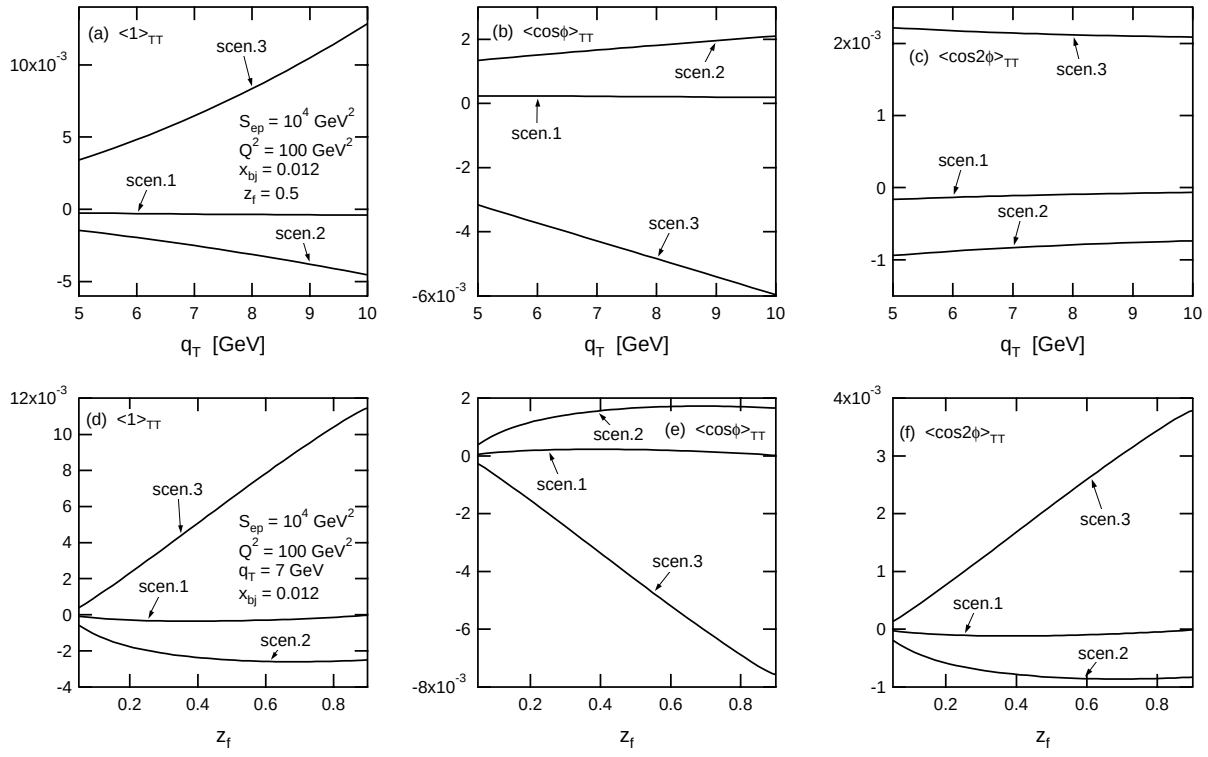

Figure 8: The same as Fig. 7 but for EIC energy.